

diffractometer and MicroVax computer system were purchased in part with NSF funds (Grant CHE-84-02155). We thank Prof. A. L. Rheingold and D. L. Staley for their efforts in trying to solve the crystal structure of  $\text{FeCl}_3[\text{P}(t\text{-Bu})_3]$ , Prof. R. Khanna for recording the low-energy FTIR spectra, Dr. L. Bennett and L. J. Swartzendruber for the solid-state SQUID variable-temperature magnetic susceptibility study on  $[\text{PH}(t\text{-Bu})_3]_2[\text{Fe}_2(\mu\text{-OEt})_2\text{Cl}_6]$ , and Prof. S. J. Lippard, R. Beer, and R. L. Rardin for providing a copy of the nonlinear fitting program developed in Prof. Lip-

pard's group for the calculation of the antiferromagnetic coupling constant.

**Supplementary Material Available:** A description of the experimental crystallography for  $\text{FeCl}_3[\text{P}(t\text{-Bu})_3]$  and tables of complete crystal data, bond distances and angles, anisotropic displacement parameters, and hydrogen atom coordinates for  $[\text{PH}(t\text{-Bu})_3]_2[\text{Fe}_2(\mu\text{-OEt})_2\text{Cl}_6]$  (8 pages); a listing of calculated and observed structure factors for  $[\text{PH}(t\text{-Bu})_3]_2[\text{Fe}_2(\mu\text{-OEt})_2\text{Cl}_6]$  (18 pages). Ordering information is given on any current masthead page.

Contribution from the Departments of Chemistry, The University of North Carolina at Chapel Hill, Chapel Hill, North Carolina 27599-3290, and North Carolina State University, Raleigh, North Carolina 27695-8204

## Crystal Structure and Magnetic Properties of Potassium Bis(dithiooxalato)nitrosylferrate(2-), a Compound with a Sulfur-Bridged Iron Dimer

Lingqian Qian,<sup>†</sup> Phirtu Singh,<sup>†</sup> HyeKyeong Ro,<sup>†</sup> and William E. Hatfield\*<sup>†</sup>

Received July 5, 1989

A dimer of potassium bis(dithiooxalato)nitrosylferrate(2-) monohydrate formula units,  $[\text{K}_2\text{Fe}(\text{C}_2\text{O}_2\text{S}_2)_2\text{NO}\cdot\text{H}_2\text{O}]_2$ , crystallizes in the monoclinic space group  $C2/c$  with unit cell dimensions of  $a = 18.416(6) \text{ \AA}$ ,  $b = 15.800(6) \text{ \AA}$ ,  $c = 9.834(4) \text{ \AA}$ , and  $\beta = 111.26(3)^\circ$  with  $Z = 4$ . The coordination around the iron atom is distorted tetragonal pyramidal with an average basal Fe-S distance of 2.27 Å. The sixth coordination position of iron is filled by a sulfur atom from an adjacent complex ion with an Fe-S distance of 3.823 Å. The Fe-N-O fragment has an angle of 161.8(3)°, and the N-O distance is 1.148(3) Å. The loosely bound dimer exhibits surprisingly strong intramolecular antiferromagnetic interactions. The magnetic susceptibility data may be fit with a dimer model by using the exchange Hamiltonian  $H_{\text{ex}} = -2JS_1\cdot S_2$  with  $S_1 = S_2 = 1/2$  and an exchange-coupling constant of  $-23.8 \text{ cm}^{-1}$ . This is a large exchange-coupling constant in view of the long Fe-S superexchange pathway.

### Introduction

Studies have shown that sulfur atoms as bridging ligands are very effective in transmitting superexchange interactions over long distances between paramagnetic metal ions in clusters and low-dimensional systems.<sup>1</sup> To more fully understand the chemical and structural features that govern these superexchange interactions, we have undertaken a systematic study of the structural and magnetic properties of sulfur-bridged transition-metal clusters, chains, and sheets. Here, we report the crystal structure and magnetic properties of the dimer  $\text{K}_4[\text{Fe}_2(\text{C}_2\text{O}_2\text{S}_2)_4(\text{NO})_2]\cdot 2\text{H}_2\text{O}$ ,<sup>2</sup> a compound that has been found to have an unsymmetrical  $\text{Fe}_2\text{S}_2$  antiferromagnetically exchange-coupled unit with two short iron-sulfur distances and two rather long iron-sulfur distances.

### Experimental Section

**Synthesis.** Commercially available ferric chloride, potassium nitrite, and potassium dithiooxalate were used without further purification. A crystalline sample of the compound was prepared by a modification of the procedure described by Coucouvanis and co-workers.<sup>2</sup> All experimental manipulations were carried out under a nitrogen atmosphere, and deoxygenated distilled water was used.  $\text{K}_2\text{C}_2\text{O}_2\text{S}_2$  (0.047 mol) was dissolved in 20 mL of  $\text{H}_2\text{O}$ , and 20 mL of an aqueous solution of  $\text{FeCl}_3\cdot 6\text{H}_2\text{O}$  (0.015 mol) was added. The solution turned violet, and an aqueous solution of  $\text{KNO}_2$  (20 mL, 0.015 mol) was added dropwise to this violet solution. The resulting solution was maintained at 70 °C with stirring for 2 h, and the hot solution was then filtered. The green precipitate was discarded, and the green solution was cooled slowly to room temperature and then placed in a refrigerator for several days. Black crystals were obtained upon filtration, and these were recrystallized from aqueous solution. Elemental analysis and the X-ray single-crystal determination, described below, confirmed the identity of the material.

**Crystallographic Data Collection.** X-ray diffraction data were collected by using a Nicolet R3m/ $\mu$  diffractometer that was equipped with a graphite monochromator and molybdenum radiation (wavelength 0.7107 Å). Cell dimensions were obtained by least-squares fitting from 25 high-angle reflections. Systematic absences indicated that the crystal belonged to the monoclinic space group  $Cc$  or  $C2/c$ . The latter was confirmed as the correct space group by the successful refinement of the structure. Two check reflections collected after every 90 reflections revealed no unexpected variation in intensity. Of the 3238 unique re-

Table I. Crystallographic Data for  $\text{K}_4[\text{Fe}_2(\text{C}_2\text{O}_2\text{S}_2)_4(\text{NO})_2]\cdot 2\text{H}_2\text{O}$

fw 844.66	space group $C2c$
$a = 18.416(6) \text{ \AA}$	$T \approx 20 \text{ }^\circ\text{C}$
$b = 15.800(6) \text{ \AA}$	$\lambda = 0.7107 \text{ \AA}$
$c = 9.834(4) \text{ \AA}$	$\rho_{\text{obsd}} = 2.08 \text{ g cm}^{-3}$
$\beta = 111.26(3)^\circ$	$\rho_{\text{calcd}} = 2.10 \text{ g cm}^{-3}$
$V = 2667(2) \text{ \AA}^3$	$R = 0.035$
$Z = 4$	$R_w = 0.05$

Table II. Atomic Coordinates ( $\times 10^4$ ) and Isotropic Thermal Parameters ( $\text{\AA}^2 \times 10^3$ )

	x	y	z	$U^a$
K(1)	0	4656(1)	2500	38(1)
K(2)	5000	4229(1)	2500	66(1)
K(3)	4296(1)	1880(1)	252(1)	46(1)
Fe	8044(1)	1262(1)	1547(1)	33(1)
S(1)	7175(1)	1734(1)	2540(1)	36(1)
S(2)	7205(1)	190(1)	484(1)	49(1)
S(3)	8512(1)	1050(1)	-250(1)	52(1)
S(4)	8460(1)	2619(1)	1709(1)	38(1)
N	8784(1)	829(1)	2945(3)	46(1)
C(1)	6425(1)	1013(1)	2068(2)	31(1)
C(2)	6454(1)	253(2)	1115(3)	34(1)
C(3)	9119(1)	1882(2)	-159(3)	37(1)
C(4)	9105(1)	2646(2)	813(2)	32(1)
O(1)	5852(1)	1081(1)	2442(2)	42(1)
O(2)	5925(1)	-262(1)	810(2)	48(1)
O(3)	9549(1)	1924(1)	-861(2)	46(1)
O(4)	9533(1)	3249(1)	851(2)	39(1)
O(5)	9396(1)	615(2)	3680(3)	76(1)
O(6)	8609(2)	1612(2)	5948(3)	67(1)

<sup>a</sup>Equivalent isotropic  $U$  defined as one-third of the trace of the orthogonalized  $U_{ij}$  tensor.

fections recorded in the range  $3^\circ < 2\theta < 55^\circ$ , 2880 reflections having  $I > 3\sigma(I)$  were used in the structure determination. Data were corrected for Lorentz and polarization effects but not for absorption owing to a moderately low absorption coefficient ( $23.4 \text{ cm}^{-1}$ ). An isotropic sec-

- (1) (a) Hatfield, W. E. *Inorg. Chem.* **1983**, *22*, 833. (b) Marsh, W. E.; Helms, J. H.; Hatfield, W. E.; Hodgson, D. J. *Inorg. Chim. Acta* **1988**, *150*, 35. (c) Vance, C. T.; Bereman, R. D.; Bordner, J.; Hatfield, W. E.; Helms, J. H. *Inorg. Chem.* **1985**, *24*, 2905.  
(2) Coucouvanis, D.; Coffman, R. E.; Tiltingsrud, D. J. *Am. Chem. Soc.* **1970**, *92*, 5004.

<sup>†</sup>The University of North Carolina at Chapel Hill.

<sup>†</sup>North Carolina State University.

**Table III.** Bond Lengths (Å)<sup>a</sup>

Fe-S(1)	2.282 (1)	Fe-S(2)	2.275 (1)
Fe-S(3)	2.255 (1)	Fe-S(4)	2.263 (1)
Fe-N	1.690 (2)	S(1)-C-(1)	1.719 (2)
S(2)-C(2)	1.712 (3)	S(3)-C(3)	1.707 (3)
S(4)-C(4)	1.717 (3)	N-O(5)	1.148 (3)
C(1)-C(2)	1.536 (4)	C(1)-O(1)	1.231 (4)
C(2)-O(2)	1.220 (3)	C(3)-C(4)	1.546 (4)
C(3)-O(3)	1.227 (4)	C(4)-O(4)	1.227 (3)

<sup>a</sup> Potassium atoms coordinate to oxygen atoms with an average distance of 2.78 Å. The shortest distance between potassium atoms is 4.103 (1) Å.

**Table IV.** Bond Angles (deg) Involving Iron

S(1)-Fe-S(2)	88.6 (1)	S(1)-Fe-S(3)	155.6 (1)
S(2)-Fe-S(3)	85.3 (1)	S(1)-Fe-S(4)	86.1 (1)
S(2)-Fe-S(4)	153.4 (1)	S(3)-Fe-S(4)	88.9 (1)
S(1)-Fe-N	105.6 (1)	S(2)-Fe-N	106.6 (1)
S(3)-Fe-N	98.8 (1)	S(4)-Fe-N	100.0 (1)
Fe-S(1)-C(1)	106.7 (1)	Fe-S(2)-C(2)	107.1 (1)
Fe-S(3)-C(3)	105.9 (1)	Fe-S(4)-C(4)	105.4 (1)
Fe-N-O(5)	161.8 (3)		

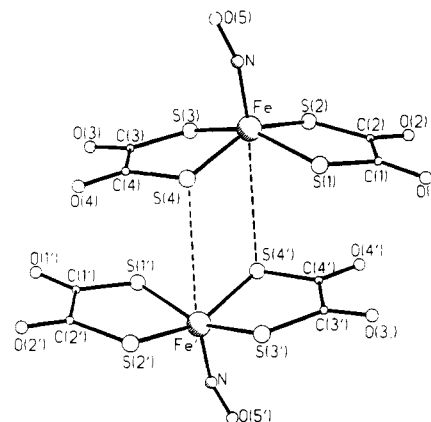
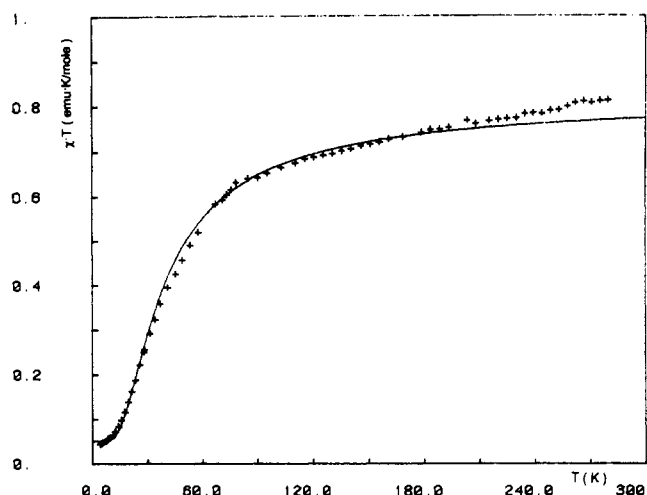
ondary extinction correction was made (secondary extinction coefficient  $6.4 \times 10^{-7}$ ). Atomic scattering factors for all atoms were taken from ref 3. Pertinent crystal data, details of data collection, and refinement parameters are summarized in Tables I and SI (supplementary material).

**Refinement of the Structure.** The iron, potassium, and sulfur atoms were located by the direct methods program SOLV of the crystallographic program package SHELXTL.<sup>4</sup> The remaining non-hydrogen atoms were found by conventional difference Fourier techniques to give a trial structure. The structure was refined by the block-diagonal least-squares technique using SHELXTL on a Data General Microelipse computer. The quantity minimized was  $\sum w(\Delta F)^2$ , where  $w = 1/(\sigma_F^2 + 0.00042F^2)$ . The non-hydrogen atoms were refined with anisotropic temperature factors. No attempt was made to place the hydrogen atoms, since the final difference Fourier map did not show clear hydrogen peaks. The refined structure was plotted by using the SHELXTL graphics package. Anisotropic temperature factors and calculated and observed structure factors are available as supplementary material. Atomic positions, bond lengths, and bond angles are given in Tables II-IV and SIII (supplementary material).

**Magnetic Measurements.** Magnetic susceptibility data from 4 to 80 K were collected by using a Princeton Applied Research Model 155 Foner vibrating-sample magnetometer with procedures that have been described earlier.<sup>5</sup> The magnetometer was calibrated with  $\text{HgCo}(\text{NC}_2\text{S}_4)$ .<sup>6,7</sup> Samples of the standard and the compound under study were contained in precision-milled Lucite sample holders. Approximately 150 mg of each were used. Magnetic data from 80 to 280 K were collected by using a Faraday system that was calibrated with  $\text{HgCo}(\text{NCS})_4$ . Corrections for the diamagnetism of the constituent atoms were estimated from Pascals constants.<sup>8,9</sup>

**Spectral Determinations.** Electron paramagnetic resonance spectra at X-band frequency of a powdered sample were recorded at a number of temperatures between 5 and 300 K with a Varian Instruments E109 EPR spectrometer equipped with a continuous-flow helium cryostat.

An infrared spectrum of a powdered sample in a KBr pellet recorded on a Beckman 4250 spectrometer exhibited a band at  $1665 \text{ cm}^{-1}$ , which may be attributed to the N-O stretching vibration. The ultraviolet-visible spectrum, which was recorded on a methanol solution by using a HP8450 UV/vis spectrophotometer, exhibited bands at 14 800, 24 000, 31 700, 37 500, 45 900, and 49 000  $\text{cm}^{-1}$ . The bands at 37 500 and 49 000 are likely ligand-based transitions, since the spectrum of  $\text{K}_2\text{C}_2\text{O}_2\text{S}_2$  in methanol exhibited bands at 38 900 and 48 800  $\text{cm}^{-1}$ .

**Figure 1.** ORTEP diagram of the dimeric structure of  $\{\text{K}_2[\text{Fe}(\text{C}_2\text{O}_2\text{S}_2)_2\text{NO}]\}_2$ .**Figure 2.** Magnetic behavior of  $\{\text{K}_2[\text{Fe}(\text{C}_2\text{O}_2\text{S}_2)_2\text{NO}]\cdot\text{H}_2\text{O}\}_2$ . The solid line corresponds to the best fit of the dimer model to the experimental data designated by +'s.

## Results

**Description of the Structure.** The structure of the complex anion  $[\text{Fe}(\text{C}_2\text{O}_2\text{S}_2)_2\text{NO}]^{2-}$  is shown in Figure S1 (supplementary material). There are no unusual aspects of the structure other than the bent nature of the Fe-N-O fragment of the molecular ion. The average Fe-S distance in the plane of the tetragonal pyramid is 2.27 Å, and the cis-S-Fe-S angles range from 85.3 (1) to 88.9 (1)°. The iron atom is 0.5 Å above the best basal plane formed by the four sulfur atoms. Thus, the trans-S-Fe-S angles are 153.4 (1) and 155.6 (1)°. The apical position of the tetragonal pyramid is occupied by the nitrogen atom of the nitrosyl ligand with an Fe-N distance of 1.690 (2) Å. The N-O bond distance is 1.148 (3) Å, and the Fe-N-O angle is 161.8 (3)°.

As shown in Figure 1, two symmetry-related  $\text{Fe}(\text{C}_2\text{O}_2\text{S}_2)_2\text{NO}^{2-}$  complex anions form a loosely bound dimer. An iron ion in one of the dianions is weakly bonded to the sulfur S(4') in the neighboring dianion. The Fe-S(4') distance is 3.823 Å, and the Fe-S(4')-Fe angle is 104.8°. Within the dimer, the Fe-Fe' distance is 4.915 Å, and the shortest interdimer Fe-Fe distance is 6.331 Å.

There are two noteworthy features of the structures. First, even though the iron is semicoordinated to a sulfur atom of a neighboring dianion, the iron is displaced 0.5 Å from the plane of four sulfur atoms toward the apical nitrosyl ligand. A comparable displacement has been found in the analogous dianionic complex  $[\text{Fe}(\text{C}_2[\text{CN}]_2\text{S}_2)_2]^{2-}$ .<sup>10</sup> Second, the iron-sulfur linkage that binds two anionic fragments into the dimer is rather long, but as noted in the following section, there is substantial intradimeric exchange

- (3) *International Tables for X-ray Crystallography*; Kynoch Press: Birmingham, England, 1974; p 71.
- (4) *SHELXTL*; X-Ray Instruments Group, Nicolet Instrument Corp.: Madison, WI 53711, 1983.
- (5) Corvan, P. J.; Estes, W. E.; Weller, R. R.; Hatfield, W. E. *Inorg. Chem.* **1980**, *19*, 1297.
- (6) Figgis, B. N.; Nyholm, R. S. *J. Chem. Soc.* **1958**, 4190.
- (7) Brown, D. B.; Crawford, V. H.; Hall, J. W.; Hatfield, W. E. *J. Phys. Chem.* **1977**, *81*, 1303.
- (8) Figgis, B. N.; Lewis, J. In *Modern Coordination Chemistry*; Lewis, J., Wilkins, R. L., Eds.; Interscience: New York, 1960; Chapter 6.
- (9) Weller, R. R.; Hatfield, W. E. *J. Chem. Educ.* **1979**, *56*, 652.

- (10) Rae, A. I. M. *Chem. Commun.* **1967**, 1245.

coupling. The significance of these observations will be explored in the Discussion.

**Magnetic Properties.** Magnetic susceptibility data were collected in the temperature range 4.2–280 K, and the data are shown as  $\chi_M T$  versus temperature in Figure 2. A maximum in magnetic susceptibility versus temperature plot, which is characteristic of antiferromagnetic interactions, occurs at approximately 40 K. In view of the structural features, which include pairs of tetragonal pyramidal  $[\text{Fe}(\text{C}_2\text{O}_2\text{S}_2)_2(\text{NO})]^{2-}$  dianions loosely bound into dimers with long Fe–S(4') semicoordinate bonds, it is reasonable to conclude that the antiferromagnetic interaction is intradimeric in nature. Assuming isotropic exchange, the exchange Hamiltonian is  $H_{\text{ex}} = -2JS_1 \cdot S_2$  with  $S_1 = S_2 = 1/2$ , and the magnetic susceptibility per mole of dimer is given by<sup>11</sup>

$$\chi_M = (2Ng^2\mu_B^2/k_B T)[3 + \exp(-2J/k_B T)]^{-1}(1 - \delta) + (Ng^2\mu_B^2/2k_B T)\delta$$

where the symbols have their usual meaning. This expression includes a correction for a monomeric impurity with 100 $\delta$  being the percent of that impurity. A least-squares fit of the magnetic susceptibility equation to the data using a nonlinear Simplex fitting routine yielded  $J = -23.8 \text{ cm}^{-1}$ ,  $g = 2.09$ , and  $\delta = 6.2\%$ . The percent impurity is probably high because a spin  $S = 1/2$  was used in the calculations. If the impurity were high-spin iron(III) with  $S = 5/2$ , then  $\delta$  would have been only 0.5%. The solid line shown in Figure 2 was generated with these best-fit parameters.

The EPR spectrum of the powdered sample at a number of temperatures ranging from 5 to 300 K consisted of a broad line centered at  $g = 2.061$ . Unexpectedly, at low temperatures where the population of paramagnetic triplet states is low, thus yielding a near-diamagnetic host for the triplet states present, there were no features on the band arising from superhyperfine interactions. Presumably, the presence of the paramagnetic impurity augmented by the Boltzmann population of triplet states leads to a mechanism for broadening the resonance line and obscures the expected superhyperfine from the nitrogen atom. The  $g$  value obtained from the magnetic susceptibility data is in good agreement with the EPR  $g$  value and lends support for the model selected for the analysis of the magnetic susceptibility data.

## Discussion

**Structural Aspects.** The nature of the bonding of NO, NO<sup>+</sup>, and NO<sup>-</sup> to transition-metal ions has been of interest for many years.<sup>12</sup> The short Fe–N bond length of 1.690 (2) Å indicates a strong covalent bond between iron and the nitrosyl ligand, although the bond is 0.13 Å longer than the corresponding bond in  $[\text{Fe}(\text{C}_2[\text{CN}]_2\text{S}_2)_2\text{NO}]^{2-}$ .<sup>10</sup> The N–O bond length in  $[\text{Fe}(\text{C}_2\text{O}_2\text{S}_2)_2\text{NO}]^{2-}$  is also longer than that in the dithiolene complex anion, it being 1.148 (3) Å in the former and 1.06 Å in the latter. These metrical parameters lead to interesting considerations. The N–O bond length in N–O<sup>+</sup> is 1.06 Å,<sup>13</sup> while the comparable bond

length in NO(g) is 1.15 Å.<sup>13</sup> The lengthening of the N–O bond in the complex dianion may be easily understood in terms of highly effective dative  $\pi$  bonding from the filled  $d_{xz}, d_{yz}$  orbitals to the unfilled  $\pi^*$  on the N–O ligand. Effective overlap is enhanced by the bent nature of the Fe–N–O fragment, which brings the  $\pi^*$  orbitals in close contact with the filled  $\pi$  orbitals on the iron ion. The influence of dative  $\pi$  bonding in N–O is further reflected by the relatively low N–O vibrational frequency of 1665  $\text{cm}^{-1}$ . The frequency of the N–O stretching vibration in N–O<sup>+</sup> is 2150–2400  $\text{cm}^{-1}$ .<sup>13</sup>

The relatively short Fe–N bond length of 1.69 Å is indicative of a strong iron–nitrogen bond, a conclusion that is supported by the 0.5-Å displacement of the iron from the plane of the four sulfur donor atoms toward the apical nitrogen atom. The long Fe–S(4') semicoordinate bond becomes important in this regard. Even though this semicoordinate bond is responsible for consociating neighboring tetragonal pyramidal complex ions into loosely held dimeric units, this bonding arrangement is of secondary importance when compared to the bonding attraction between the iron and the nitrosyl ligand.

**Exchange-Coupling Mechanism.** In view of the long iron–iron distance of 4.915 Å in the bimetallic exchange-coupled unit, it is reasonable to conclude that direct exchange, resulting from overlap of magnetic orbitals on the iron ions, contributes little to the exchange-coupling mechanism. Rather, the exchange coupling occurs by a superexchange mechanism that operates through the orbitals of the bridging sulfur atoms. In this regard it is important to establish the identity of the magnetic orbitals. An early EPR study<sup>14</sup> of liquid and frozen solutions of  $[\text{Fe}(\text{C}_2\text{O}_2\text{S}_2)_2\text{NO}]^{2-}$  in methylene chloride or a methanol–glycerol mixture led to the conclusion that the unpaired electron was in either the  $d_{z^2}$  or the  $d_{xz}$  orbital, with the probability of it being in  $d_{z^2}$  being more likely.

To address the problem of the identity of the magnetic orbital, we carried out an extended Hückel calculation<sup>15</sup> on a monomer fragment. Since the monomer fragment has no symmetry, there are contributions from several orbitals to the HOMO, but the major contributions, by far, are from iron 3d<sub>z<sup>2</sup></sub> and 4p<sub>z</sub>. These orbitals overlap effectively with the orbitals of the bridging sulfur atom, and this overlap results in the relatively large superexchange interaction.

The charge distribution in the dianion resulting from the Hückel calculation is  $[\text{Fe}^0(\text{C}_2\text{O}_2\text{S}_2)_2^{-1.67}(\text{NO})^{-0.33}]$ . Thus, the low N–O stretching vibration of 1665  $\text{cm}^{-1}$  and the bond length of 1.15 Å may be understood in terms of the partial negative charge on NO.

**Acknowledgment.** This research was supported by the National Science Foundation through Grant No. CHE 88 07498.

**Supplementary Material Available:** Figure S1, showing the monomeric unit, and Tables SI–SIV, listing details of the structure determination, thermal parameters, and angles in the dithiooxalate ligand (5 pages); a table of calculated and observed structure factors (19 pages). Ordering information is given on any current masthead page.

- (11) Hatfield, W. E. In *The Theory and Applications of Molecular Paramagnetism*; Boudreaus, E. A., Muly, L. N., Eds.; John Wiley & Sons, Inc.: New York, 1976; Chapter 7, p 358.  
 (12) McCleverty, J. A. *Progress in Inorganic Chemistry*; Cotton, F. A., Ed.; John Wiley and Sons: New York, 1968; Vol. 10.  
 (13) Cotton, F. A.; Wilkinson, G. *Advanced Inorganic Chemistry*, 4th ed.; John Wiley and Sons: New York, 1980; Chapter 13, p 424.

- (14) Sweeney, W. V.; Coffman, R. E. *J. Phys. Chem.* **1972**, *76*, 49.  
 (15) Howell, J.; Rossi, A.; Wallace, D.; Haraki, K.; Hoffmann, R. *Forticon8*; Quantum Chemistry Program Exchange, Indiana University: Bloomington, IN; QCPE344.